Simulations of Heat Loads on Plasma Facing Components

M. Airila 1), O. Dumbrajs 1), J. Heikkinen 2), S. Karttunen 2), T. Kiviniemi 1), T. Kurki-Suonio 1), S. Lehto 2), J. Likonen 2), J. Lönnroth 1), K. Rantamäki 2), S. Saarelma 1), R. Salomaa 1), S. Sipilä 1), T. Tala 2)

Euratom-TEKES Association
1) Helsinki University of Technology, P.O. Box 2200, FIN-02015 HUT, Finland
2) VTT Processes, P.O. Box 1608, FIN-02044 VTT, Finland

E-mail address of main author: samuli.saarelma@hut.fi

Abstract: Three important phenomena affecting heat loads on plasma facing components in a tokamak are simulated. The simulations using the guiding centre orbit following code ASCOT show that the observed heat load asymmetry between inner and outer divertor can be explained with a radial electric field in the scrape-off layer (SOL). Additionally, the observed disappearance of sharp load peaks in helium plasmas can be explained by mass difference between helium and deuterium. The differences in ELM size and, consequently, in divertor heat load, between the type I and type II ELMs are explained analysing the MHD stability of the edge plasma with self-consistent bootstrap current. The ELM triggering peeling instability becomes narrower in type II ELMy plasma leading to a smaller ELM loss than in type I ELMy plasma. The hot spot formation from parasitic absorption in front of an LH grill that is a problem in present day tokamaks is simulated using a PIC (particle-in-cell) code using ITER parameters. The ITER configuration shows no parasitic absorption.

1. Introduction

The most critical components of a fusion reactor will be the solid surfaces that come into contact with the hot fusion plasma. In this work, three important phenomena affecting the heat loads on the targets are analysed in detail. The The edge ion heat transport to the targets through the SOL region and the heat load asymmetry on the divertors in particular were simulated using the orbit following code ASCOT. The ELMs are analysed with respect to plasma edge MHD stability changes when moving from the standard H-mode type I ELMs to small and benign type II ELMs. Finally, the hot spot formation in LH-grills is modelled using PIC-simulations.

2. Studies of Divertor Target Load Profiles

Extending the lifetime of the divertor targets is one of the key questions in the design and operation of ITER. Understanding the various mechanisms affecting the particle and energy load distribution on divertor targets is important for the optimisation of divertor design and of SOL parameters. Parameters such as the edge plasma and SOL radial electric field E_r, the direction of the ∇B drift, density and temperature of the pedestal as well as the poloidally asymmetric plasma and neutral density and temperature profiles in the SOL can all have an effect on the distribution of particle and heat fluxes on the divertor targets [1,2].

JET divertor load measurements using embedded thermocouples have indicated a large inner/outer target load asymmetry and a significant non-uniformity in the load to the outer target [3]. Furthermore, under H-mode conditions, the load appears to be dominated by the ion component. While the inner/outer target load asymmetry can be understood in terms of the conventional fluid picture, the sharp structures in the deposition profile as well as the ion dominance of the load can not be readily explained by the fluid approach.

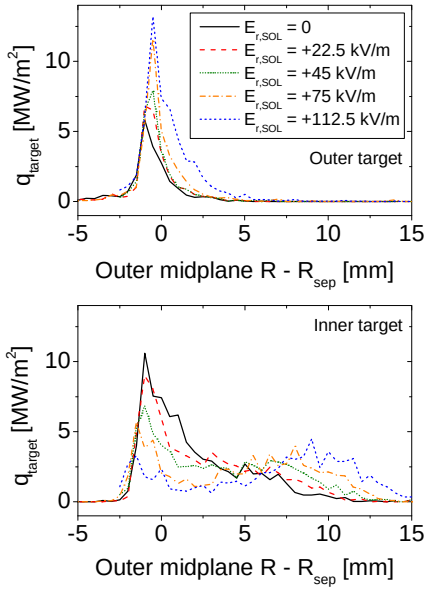

Fig. 1. *Effect of SOL E_r on divertor target ion loads.*

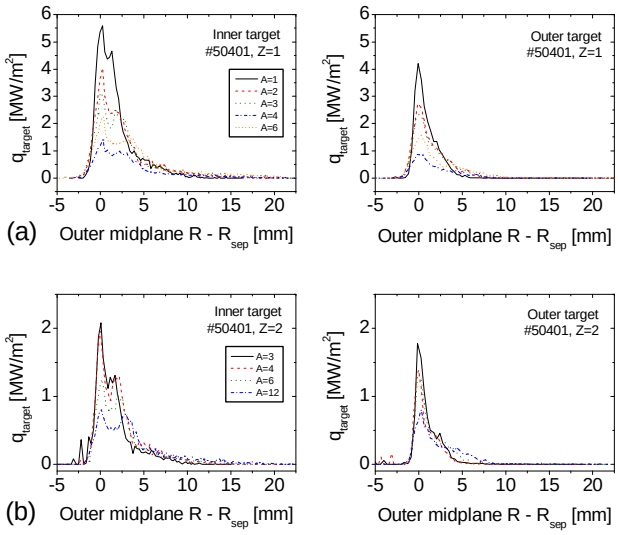

Fig. 2. *Simulated target ion load profiles for JET discharge #50401 at t = 54 s. a) for ions with charge Z=1. b) for ions with Z=2. No sharp load peak typical of*

We have made a wide range of simulations varying the parameters likely to affect the target load profiles simulating the target loads with the guiding centre orbit following Monte Carlo code ASCOT. We were able to reproduce the strongly peaked structure of the load profiles and the SOL radial electric field emerged as a likely candidate for explaining the observed load asymmetry between the inner and the outer target (see Fig. 1). The asymmetry shifts outwards with increasing SOL E_r.

In similar helium discharges with only type III ELMs present, no sharp peak in the target load profile has been experimentally observed in JET [4]. The observations from helium plasmas could be interpreted as evidence that type I ELMs might be responsible for the load peaking. To propose another explanation for the observations, we applied ASCOT to study the ion load profile differences arising directly from the effects of ion species mass and charge. SOL radial electric field was not modelled in this parameter scan. The results are shown in Fig. 2 which demonstrates the effect of ion mass A and charge Z: orbit losses are effectively quenched by the higher ion-ion collisionality and lower thermal velocity of helium (A=4, Z=1 or 2) as compared to deuterium (A=2, Z=1) when all other parameters are the same.

3. MHD Stability Analysis of Type II ELMs

The main operation mode of ITER-FEAT will be the ELMy H-mode. However, in standard Type I ELMy H-mode, the divertor erosion may become unacceptably high. Comparable confinement conditions can be achieved with smaller but more frequent Type II ELMs [5]. Experimentally, Type II ELMs have been observed in plasmas with higher triangularity [6,7], higher density[6,7], high edge safety factor (q_{95})[7] and almost double null configuration [7], as compared with the Type I ELMs. While the fundamental understanding of the ELM phenomenon is still not known, several models have been presented to explain it [8]. Here, we use a model presented by Connor et al. [9] for type I ELMs as a working model. In the model, an ELM is triggered by a peeling-ballooning mode. An MHD stability analysis is conducted to investigate how the character of bootstrap current-driven peeling modes and the pressure driven ballooning modes change with the plasma conditions from type I to type II ELMy

plasmas. We include all the experimentally observed factors in the stability analysis and study each of them independently using GATO [10] for peeling modes with low and intermediate toroidal mode number ($n < 9$) and, IDBALL for $n=\infty$ ballooning modes.

We find in the stability analysis that high triangularity and high q_{95} not only make the plasma more stable against the peeling modes (i.e. higher bootstrap current is needed to destabilise the mode), but also the mode structure becomes more localised at the edge (Fig 3.). The changes to the ballooning stability were very small. If the collisionality is low, the edge bootstrap current lowers the edge shear and enables the plasma to access second stability. Plasma shaping and safety factor variation do not change this behaviour.

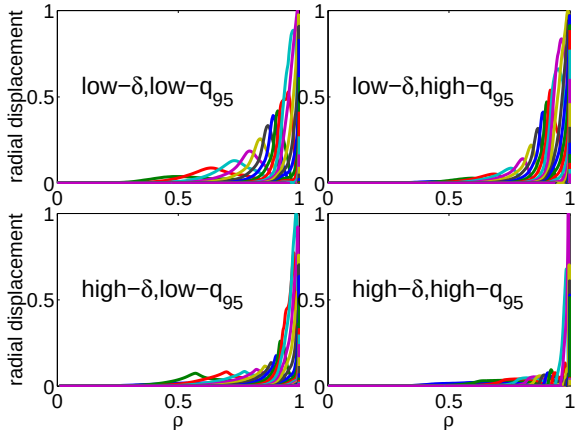

Fig. 3. *The radial mode structure of the n=3 peeling mode changes when the triangularity is increased from 0.15 to 0.45 and q_{95} from 4 to 5.*

The second stability access in the low collisional edge plasma enables the pressure gradient to increase without limit until the low-n peeling mode was triggered. Increasing density while keeping the pressure fixed, results in higher collisionality and, consequently, lower bootstrap current. The lowered edge current increases the shear and closes the second stability access for ballooning modes. On the other hand, the peeling modes that are destabilised by the edge bootstrap current become more stable. As a result of these two effects plasma will never become low-n peeling mode unstable, since the ballooning modes limit the pressure gradient and the bootstrap current does not rise to the value required for the destabilisation. Instead, the plasma edge becomes destabilised by an intermediate-n peeling-ballooning mode with a very narrow mode width.

In an x-point, the poloidal magnetic field is zero and, thus, the shear is increased in its vicinity. Normally a tokamak plasma has a single x-point. Moving a second x-point close to the separatrix has been observed to have a strong effect on the ELMs [7]. First, the pure type I ELMs are changed to a combination of type I and type II ELMs and as the second separatrix comes even closer, pure type II ELMs are observed. The second x-point has a significant effect also on the equilibrium and the plasma stability. The increased shear near the second x-point has a stabilising effect on the low-n peeling modes. The second x-point stabilises the low-n peeling modes regardless of the plasma triangularity. The second x-point also makes the mode narrower. The second x-point has little effect on the ballooning modes, because they are localised on the low field side and the x-points are on the top and bottom of the plasma. The shape of the plasma changes slightly with the second x-point and this widens the second stability access. However, the increased density still closes the second stability access.

The stability property changes can be combined to explain the experimentally observed change from large amplitude type I ELMs to smaller type II ELMs. The linear stability analysis gives only the mode structure and the growth rate of the instability. Non-linear simulations would be needed to determine the exact plasma response after the instability is triggered. However, it is reasonable to assume the ELM size (how much energy and particles is expelled from the plasma) is proportional to the width of the triggering instability. A schematic picture of the ELM cycle change is shown in Fig. 4. The improved stability against the low-n peeling modes by high triangularity, high q_{95} and almost double null configuration

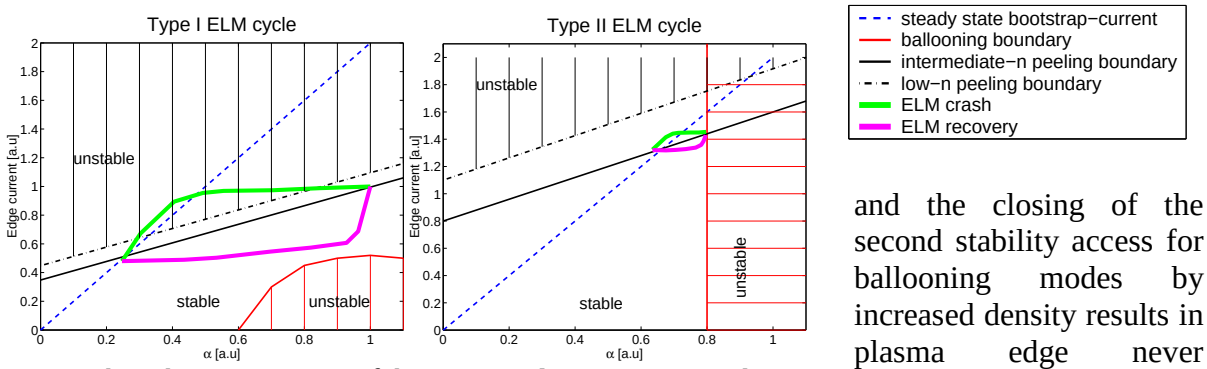

Fig. 4. *The schematic picture of the type I and type II ELM cycles and the MHD stability boundaries in the edge region. The steady-state bootstrap current represents the edge current that is reached, if no instabilities are triggered.*

and the closing of the second stability access for ballooning modes by increased density results in plasma edge never reaching the low-*n* peeling mode stability boundary. The ELM is triggered by intermediate-*n* modes that are destabilised by lower pressure gradient and have a narrower mode width than low-n modes. Because of the narrow width, the ELM losses are smaller than an ELM triggered in plasma with low triangularity, low q_{95}, single null and low density where in addition to the narrow intermediate-*n* modes, also the wide low-*n* modes become unstable. The increased resisitivity in type II ELMy plasmas increases the current diffusion. This makes the edge current recovery after an ELM crash faster and, thus, increases the ELM frequency.

4. Heat Loads on the LH Grill Limiters

In addition to the heat loads due to the ELMs, a more stationary type of heat load can be found. On components that are magnetically connected to the lower hybrid grill, strong localised heat loads have been observed [11]. It is assumed that these hot spots are caused by parasitically accelerated electrons [12]. With parasitic absorption we here mean the absorption of the very high $n_{||}$ part of the LH power spectrum at the grill mouth. Particle-in-cell simulations with Tore Supra parameters indeed confirm the acceleration of the electrons.

We investigated the parasitic absorption of LH power in the edge plasma in front of the ITER lower hybrid launcher with PIC simulations. The PIC method makes it possible to solve the electric field self-consistently providing information of the absorbed power, the radial deposition profiles and the absorption length. The electrostatic PIC code XPDP2 [13] used in this work is two-dimensional in configuration space and three-dimensional in velocity space.

We performed altogether six simulations for ITER parameters. The density in front of the antenna was n_e=6.2×10^{18} m^{-3}. A linear density profile was used with a density scale length of 1 cm. The magnetic field lying along the *z*-axis was B=4 T. The frequency of the grill was f = 5 GHz. The initial electron temperature ranged from 25 to 100 eV and the coupled power density varied from 14 to 55 MW/m^2. The width of an active waveguide was 9.25 mm and the one of a passive waveguide was 7.25 mm. The width of the wall between the waveguides was 3 mm. The phase difference between the active waveguides is 3π/2. The feeding phase between the 8 waveguides multijunction is 0.

In order to model experiments with realistic wave spectra we obtained the surface charge from the SWAN [14] calculations. The charge density is very peaked at the walls between the waveguides. Most of the power is in the main peak of the spectrum at $n_{||} \approx 2$. However, a

small amount of the power is in the very high modes, which may cause significant electron heating and consequently, hot spots on the limiter [12,15].

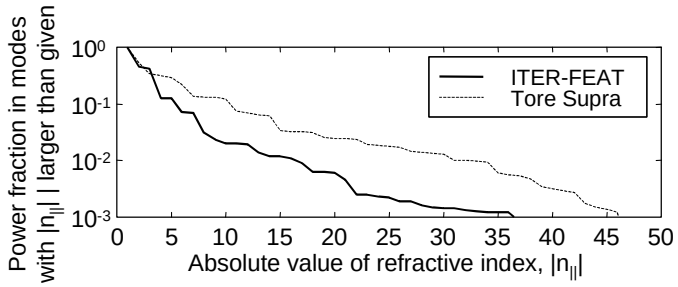

Fig. 5. *Power content in the higher $n_{||}$ modes for ITER and TS grills.*

The design of the ITER LH grill has significantly reduced the power content in the high-$n_{||}$ modes (Fig 5). We have here compared the spectra for ITER and the one for the Tore Supra launcher C3. One should note that the densities in front of the launchers are different in each case. For ITER the density is n_e=6.2×10^{18} m^{-3} but for Tore Supra only 10^{18} m^{-3}. However, the density dependence of the power fraction in the high-$n_{||}$ modes should not be that pronounced and the power fraction in the highest modes should increase with the density. At least this was the case for the Tore Supra launcher.

The PIC simulations performed for the ITER LH grill confirm the predictions from the SWAN calculations. The power content in the high-$n_{||}$ modes is apparently so low that in the ITER case no absorption was observed. For all the ITER cases with $14 < I_{in} < 55$ MW/m^2 and $25 < T_e < 100$ eV, the absorbed power density was negligible. This was also seen in the velocity distributions where no changes were seen.

Conclusions

The simulations showed that the radial electric field in the SOL is a likely candidate for explaining the observed load asymmetry between the inner and the outer divertor target. The asymmetry is avoided in helium plasmas due to the effects of ion species mass and charge on the ion-ion collisionality and ion thermal velocity. The MHD stability analysis shows narrowing of the eigenfunction of the triggering peeling instability. This can explain the small type II ELMs. The PIC simulations for ITER LH launcher confirm the predictions that the parasitic absorption is negligible.

References

[1] STANGEBY, P.C., CHANKIN, A.V., Nucl. Fusion **36** (1996) 839.
[2] CHANKIN, A.V. et al., Contrib. Plasma Phys. **40** (2000) 288.
[3] MATTHEWS, G.F. et al., J. Nucl. Mater. **290–293** (2001) 668.
[4] PITTS, R.A. et al., "Comparing Scrape-Off Layer and Divertor Physics in JET Pure He and D Discharges". 15th Int. Conf. on PSI, 27-31 May, 2002, Gifu, Japan. To appear in the Proceedings.
[5] OZEKI, T. et al, Nucl. Fusion, **30** (1990), 1425.
[6] LEONARD, A.W. et al, J. Nucl. Mater. **290-293** (2001) 1097.
[7] STOBER, J. et al, Nucl. Fusion **41** (2001), 1123.
[8] CONNOR, J.W., Plasma Phys. and Contr. Fusion, **40** (1998), 191.
[9] CONNOR, J.W., HASTIE, R.J., WILSON, H.R., Physics of Plasmas, **5** (1998), 2687.
[10] BERNARD, L.C., HELTON, F. J., Moore, R. W., Comp. Phys. Comm. **24** (1981) 377.
[11] MAILLOUX, J. et al., J. Nucl. Mater. **241-243** (1997) 745.
[12] FUCHS, V., et al., Phys. Plasmas **3** (1996) 4023.
[13] VAHEDI, V., BIRDSALL, C.K., et al., Phys. Fluids, **B5,** (1993) 2719.
[14] MOREAU, D., GORMEZANO, C., MELIN, G., NGUYEN, T., in Rad. in Plasmas, vol. 1, (B. McNamara, ed.), (World Scientific, 1984) 331.
[15] RANTAMÄKI, K.M., et al., Nucl. Fusion **40** (2000) 1477.